# Rapid and intense phosphate desorption kinetics when saltwater intrudes into carbonate rock

Hilary Flower[1], Mark Rains[1], David Lewis[2], and Jia-Zhong Zhang[3]

[1]School of Geosciences, University of South Florida
4202 E. Fowler Avenue, NES 107
Tampa, Florida 33620, USA
E-mail: hflower@mail.usf.edu; mrains@usf.edu

[2]Department of Integrative Biology, University of South Florida
4202 E. Fowler Avenue, SCA 110
Tampa, Florida 33620, USA
E-mail: davidlewis@usf.edu

3Atlantic Oceanographic and Meteorological Laboratory
National Oceanic and Atmospheric Administration
4301 Rickenbacker Causeway
Miami, Florida 33149, USA
E-mail: jia-zhong.zhang@noaa.gov

*Estuaries and Coasts*

**Abstract**

It is important to understand how phosphate sorption dynamics of coastal carbonate aquifers are affected by seawater intrusion, because many coastal aquifers are composed of carbonate rocks and subject to an increase in saltwater intrusion during relative sea-level rise. Twelve carbonate rock and unconsolidated sediment specimens were acquired from a test corehole spanning the full thickness of the Biscayne aquifer in southeastern Florida. All 12 samples exhibit low phosphorus content but variable contents of iron. Column leaching experiments were conducted with two carbonate aquifer samples, alternating between freshwater and saltwater flow. With the first influx of saltwater, phosphate concentration in leachate increased rapidly from a freshwater value of approximately 0.2 µM to peaks of between 0.8 and 1.6 µM. The phosphate concentration began to diminish as saltwater continued to flow, but sustained desorption continued for over 2 hours. Overall, seawater drove sorption behavior much more than chemical rock composition for the aquifer rocks and sediment from the seven rock samples for which we did isotherm sorption experiments. Our results indicate that an immediate and intense pulse of phosphate desorption from carbonate rock and sediment with low phosphorus content occurs in response to an influx of seawater, and that the duration of desorption will vary by layer within a single aquifer.

**Key words: Florida Everglades, groundwater, submarine groundwater discharge**

## Introduction

Brackish groundwater discharge is an important contributor to coastal estuary nutrient budgets. In some regions it is orders of magnitude higher in phosphorus concentration than overlying surface water (Slomp and Van Cappellen 2004). Many coastal ecosystems are phosphorus limited, and phosphorus supply from groundwater discharge can affect coastal

ecosystems (Moore 1999). Brackish groundwater is commonly enriched in phosphorus because freshwater-saltwater mixing can release phosphate from aquifers composed of carbonate rocks through phosphate desorption and mineral dissolution.

In many coastal areas, saltwater intrusion has increased in recent decades owing to factors that reduce the hydraulic gradient, such as groundwater abstraction, sea-level rise, and drainage resulting from seepage from canals (Barlow and Reichard 2010). Conversely, recharge of the aquifer can cause the saltwater intrusion front to retreat seaward. These movements of the freshwater-saltwater interface trigger geochemical reactions. An incursion of saltwater into a part of the aquifer that had been immersed in freshwater could cause phosphate (the bioavailable form of phosphorus) to desorb from mineral surfaces and raise ambient water phosphate concentrations, while a seaward retreat of the saltwater intrusion front could cause phosphate to adsorb to aquifer bedrock due to freshening.

Saltwater intrusion has occurred in the carbonate aquifers of many coastal regions, such as Florida, USA (Fitterman 2014), Mallorca, Spain (Price and Herman 1991), and Apulia, Italy (Cotecchia et al. 1974). For coastal ecosystems affected by groundwater discharge, the ecological impact of saltwater-induced phosphate desorption depends upon the degree to which desorption raises ambient water phosphate concentrations. In turn, this is affected by both kinetic factors (e.g., the rate and duration of desorption) and equilibrium factors (e.g., the buffering capacity of the aquifer rocks). The existing kinetic studies of saltwater-induced desorption from carbonate minerals have shown significant phosphate release, but all such studies involved a preliminary step of artificially loading the mineral surfaces with phosphate (Corbett et al. 2000; Millero et al. 2001; Price et al. 2010). Although some aquifers have an anthropogenic source of phosphate, such as parts of the Florida Keys subject to sewage injection (Corbett et al. 2000),

other carbonate aquifers have very low phosphorus content (Flower 2016). It would be important to know whether or not aquifers depauperate in phosphate can desorb enough phosphate to raise ambient groundwater concentrations to ecologically significant concentrations.

Our hypothesis is that seawater-induced phosphate desorption does occur within carbonate coastal aquifers that have low to moderate phosphorus content. Our conceptual model is that phosphate desorption would vary with depth in a given aquifer due to variable chemical composition among rock layers. The chemical content of a mineral surface can strongly affect how efficiently phosphate adsorbs in freshwater, and the extent to which saltwater weakens this sorption efficiency, triggering phosphate desorption. In particular, phosphate adsorption/desorption behavior can be driven by the amount of iron bound to the negatively charged carbonate sites on solid calcium carbonate, as well as the amount of inorganic phosphate loosely adsorbed to the mineral surface (Zhang and Huang 2007). We predicted that a layer of rock with moderate to high phosphorus content would undergo rapid, intense and sustained phosphate desorption, and conversely that phosphate desorption would be weak and short-lived in layers with low phosphorus content.

**Approach.** The focus of this project is a kinetic study with high temporal resolution comparing phosphate desorption from two rock samples when subjected to alternating freshwater and saltwater flow. We measured the rate, magnitude and duration of saltwater-induced phosphate desorption from mineral grains in a flow column. To place the kinetic experiments in context of composition variability within the aquifer, we measured phosphorus and iron content on 12 elevations within a single test corehole spanning the full thickness of the Biscayne aquifer, of southeast Florida. To add detail to our understanding of the influence of rock composition and water type on sorption behavior, we investigated the equilibrium sorption behavior of rocks from

seven of these elevations in both freshwater and saltwater. This experimental design permitted us to compare both kinetic and equilibrium phosphate sorption behavior with respect to different rock composition and water type.

**Purpose.** The purpose of this study is to investigate how the phosphate desorption kinetics of carbonate aquifer rock may change when a saltwater intrusion front moves landward or seaward. By investigating key chemical composition characteristics and the phosphate sorption behavior of 12 compositionally variable rock specimens within the same aquifer, we aim to shed light on the potential variability of phosphate desorption within a single aquifer. The results of this study will provide critical information for water management and restoration efforts in carbonate coastal regions undergoing saltwater intrusion and brackish groundwater discharge to coastal estuaries.

**Description of study area.** The Biscayne aquifer is the upper part of the surficial aquifer system in Miami-Dade County and extends through the central and eastern part of the Everglades National Park (Figure 1). At the eastern edge of the Biscayne aquifer along the coast, saltwater intrusion has caused the abandonment of many wells (Prinos et al. 2014). At its southern edge in the Everglades National Park, saltwater has intruded between 6-28 km inland along the base of the aquifer (Price et al. 2006). The overlying ecosystem of the Everglades has been called “phosphorus starved” due to its highly oligotrophic nature and its sensitivity to even small increases of dissolved phosphorus (Noe et al. 2001). For this reason, a detailed understanding of the storage and transport of phosphorus in the Everglades has been described as “urgently needed” in order to effectively and comprehensively address water quality concerns (NRC 2014).

## Methods

**Rock samples.** We acquired 12 rock samples to investigate how phosphate sorption characteristics and key aspects of rock composition may vary with depth in a carbonate aquifer. We chose the G-3784 test corehole because it spans the full vertical thickness of the Biscayne aquifer at this location, (Figure 1), comprising three geologic formations, the Miami Limestone, the Fort Thompson Formation, and an upper part of the Tamiami Formation (which is considered semi-confining in some areas) (Cunningham et al. 2004). The G-3784 test corehole was drilled in a freshwater part of the aquifer on the berm of Levee 31N adjacent to the L-31N canal (latitude: 25°42'07.36"N; longitude: 080°29'46.26"W) as part of a seepage study by United States Geological Survey in 2003 (Cunningham et al. 2006; Cunningham et al. 2004; USGS 2003).

The G-3784 test corehole was drilled at a diameter of 4 inches using a conventional hydraulic coring method with freshwater as a drilling fluid until quartz sands were encountered (Cunningham et al. 2006). The remaining section of the borehole was drilled to the elevation of -28.59 m NAVD88 using a split-barrel sampler and standard penetration test methodology (Cunningham et al. 2006).

Lithologic descriptions are provided in Table 1 along with elevations. Using the labeled wood markers in the storage boxes (marked in feet below land surface, which we converted to meters NAVD88) we assigned elevations to the top and bottom of each specimen where possible. For some samples precise top/bottom elevation could not be determined (e.g., where the core length is shorter than the depth range indicated by markers), and instead we assigned elevations corresponding to the top and bottom of the widest interval from which they may have been extracted. Using the top/bottom elevations assigned to each rock sample we calculated a midpoint elevation for use in graphs.

Rock samples were crushed and sieved to <125 μm for composition measurements and sorption isotherm experiments. We measured four aspects of the rocks' chemical composition (described in detail below) that can be important factors for phosphate sorption behavior: Loosely adsorbed phosphate (both inorganic and organic), total sedimentary phosphorus, and iron that was bound to carbonate mineral.

Loosely adsorbed or readily exchangeable inorganic phosphate (Zhang et al. 2004), is defined as the inorganic phosphate released from rock powder by 1 M $MgCl_2$ solution at pH 8.0. In general, loosely adsorbed inorganic phosphate is considered to be the most reactive solid phosphorus species, and rocks with more loosely adsorbed inorganic phosphate have been found to desorb more phosphate (Wang and Li 2010; Zhang and Huang 2007; Zhou and Li 2001). We determined both loosely adsorbed inorganic phosphate and loosely adsorbed organic phosphate following the protocol established by Ruttenberg (1992). Loosely adsorbed organic phosphate is determined by subtracting the loosely adsorbed inorganic phosphate from the total-dissolved-phosphorus removed by $MgCl_2$, which was measured using the sub-boiling temperature protocol of (Huang and Zhang 2009).

Total sedimentary phosphorus was determined by high temperature combustion following the protocol of Zhang et al. (2004). The rock powders were placed in 100-mL Pyrex beakers and wetted with a few drops of 1 M $Mg(NO_3)_2$ solution and then ashed in a combustion furnace at 550°C for 2 hours. After the samples were cooled to room temperature, a 50 mL of 1 M HCl solution was added to each sample. The samples were then agitated at 25°C for 24 hours to extract phosphorus. Samples were filtered to remove any particulate residuals and the filtrates were analyzed for phosphate.

Iron bound to carbonate mineral surfaces has been found to enhance phosphate adsorption, especially in rocks with low amounts of loosely adsorbed inorganic phosphate (Zhang and Huang 2007). We determined the amount of carbonate-bound iron in our rock samples by dissolution of solid phase iron in 1 N HCl solution. The total dissolved iron ($Fe^{3+}$ + $Fe^{2+}$) in the solution was reduced with ascorbic acid to $Fe^{2+}$. The $Fe^{2+}$ was then spectrophotometrically determined with a ferrozine reagent in a pH 5.5 buffer solution at a maximum absorption wavelength of 562 nm (Zhang et al. 2001).

We conducted rock composition measurements first so that we could choose for subsequent experiments samples that exhibited the extremes of composition within our "snapshot" of 12 elevations. Accordingly, the seven samples chosen for isotherm experiments capture the observed range. For the two rocks chosen for column experiments, our original plan was to select the two samples bearing the lowest and highest amounts of loosely adsorbed inorganic phosphate. However, all of our rocks fell in the very low end of the range we had anticipated based on the available literature (results are presented in Figure 3 and discussed in detail in a subsequent section). We became concerned that even the two rock samples with the higher loosely adsorbed inorganic phosphate values may still have desorbed too little phosphate to be detectable in the leachate phosphate concentrations. Accordingly, we conducted column experiments on the samples with the highest loosely adsorbed inorganic phosphate from our set of 12.

**Water samples and analyses.** Whenever possible it is ideal to conduct phosphate adsorption/desorption experiments using water samples from the study area so to include the naturally occurring chemical species that may participate in the water-rock interactions in the field. We collected two water types as representatives of ambient fresh groundwater and

saltwater (sampling locations provided in Figure 1). Fresh groundwater (hereafter referred to as "freshwater") was collected from shallow monitoring well TSB-15 (Figure 1), which is screened at a depth of 4.6 m within the bedrock underlying a freshwater sawgrass marsh (Price 2001). Our saltwater sample is from Florida Bay surface water taken from a dock in Key Largo. Sulfate concentration was below detection limit in our freshwater sample and 28.4 mM in our saltwater sample. Total alkalinity, dominated by bicarbonate within our range of pH, was 4.0 and 2.9 mM for our saltwater and freshwater respectively. Procedures for determining water properties and results for these two field water samples are described in detail elsewhere (Flower et al. 2016).

In our experiments, phosphate concentrations were measured as soluble reactive phosphate the day of the completion of each experiment using the microscale malachite green method (D'Angelo et al. 2001), measuring absorbance at a wavelength of 630 nanometers in 96-well microplates on a BioTek EPOCH microplate spectrophotometer. Initial phosphate concentration for freshwater was 0.050 μM and for our saltwater was 0.076 μM.

**Column experiments.** We assembled a column apparatus (depicted in Figure 2) based on Suzumura et al. (2000). A Cole Parmer low-flow peristaltic pump was used to pump freshwater or saltwater from beakers at a rate of 1 mL $min^{-1}$ at room temperature (23 ± 0.5°C). A borosilicate glass Kimble Chase Flex-Column (inner diameter of 1.5 cm, length 20 cm) was filled with sediment or crushed rock (pore volume 10 mL). The water was pumped upward so as to minimize the formation of channels. As leachate exited the top of the flex-column, it passed through a 0.45 μm nylon syringe filter (replaced after every 30 mL) to remove particulates. A final segment of tubing delivered the leachate to a sample vial. For each leachate sample, 100 μL was pipetted twice, first to measure conductivity using a Horiba Laqua Twin conductivity meter, and second to measure pH using a Horiba Laqua Twin pH meter with a glass electrode. These

devices were chosen for their ability to measure such small volumes water, thereby making it possible for leachate samples as small as 1 mL to be tested for conductivity, pH, and phosphate. Vials were then capped so as to prevent evaporative loss. Immediately following the conclusion of the experiment, phosphate concentrations were determined as previously described.

Five column experiments were conducted, with distinguishing aspects outlined in Table 2. The first three column experiments used sample 12, from the Tamiami Formation. This sample comprised unconsolidated shells and sand, requiring no crushing for use in the column. The column was filled with 47 g sediment with variations in grain size and leaching water sample size (Table 2). The first column experiment omitted the sieving step, so as to most closely approximate the natural aquifer conditions. Inflow water alternated as follows: 60 mL of freshwater, 70 mL of saltwater, 70 mL of freshwater, 70 mL of saltwater, and 60 mL of freshwater. The first four leachate samples were 10 mL each as the sediment equilibrated to freshwater, and all subsequent samples were 2 mL each (154 samples total).

The only difference in the second column experiment was that the sediment was sieved to include only the size fraction between 1.0-1.4 mm (again 154 leachate samples total). The third column experiment differed from the previous one by two modifications for the purpose of increasing the resolution: (1) samples were 1 mL instead of 2 mL, and (2) we undertook only one influx of saltwater (sequence: 60 mL freshwater—70 mL saltwater—60 mL freshwater) so as to halve sample size without doubling the number of samples (this experiment consisted of 162 samples total) which would have exceeded the limits for same-day phosphate analysis.

In order to compare desorption across different lithology, the last two column experiments (4 and 5) were conducted using sample 8, from the Fort Thompson Formation,

crushed and sieved to 1.0-1.4 mm (Table 2). Only 44 g of these grains could fit in the column (compared to 47 for the previous sample), which could be explained by crushed grains skewing toward 1.4 mm rather than 1 mm. Column experiment 4 consisted of a single freshwater-saltwater- freshwater sequence. After observing an apparent plateau of phosphate concentration during the saltwater portion of column experiment 4, we designed our final experiment to observe sustained saltwater flow, rather than change back to freshwater. For column experiment five (Table 2), we followed an initial 60 mL flush of freshwater with 200 mL saltwater. Although a greater duration of sustained saltwater flow would have been ideal, we had to limit the duration of the column experiment so as to be able to conduct phosphate analysis on the same day.

**Sorption isotherm experiments.** Sorption isotherm batch experiments based on the methods of Froelich (1988) were conducted by combining in a 60 mL test tube 100 mg of one of the seven rock samples, 30 mL of either freshwater or saltwater, 20 μL chloroform (to prevent microbial activity from affecting phosphate concentrations), and a given measure of 3 mM phosphate stock solution to yield one of 10 different initial soluble reactive phosphate concentrations: 0.0 (none added), 0.6, 1.0, 1.3, 1.6, 1.9, 3.3, 4.8, 5.6, 6.5, and 8.1 μM. After 24 hours of shaking at 200 rpm on a platform shaker at room temperature (23 ± 0.5°C), each suspension was passed through a 0.45 μm nylon syringe filter. The filtrate was immediately analyzed for final soluble reactive phosphate concentration, as described previously.

**Sorption isotherm parameters.** Many different aspects of how phosphate behaves given a combination of a particular rock powder and a particular water type can be learned by simply measuring the amount of phosphate adsorbed in solutions with a range of initial phosphate concentrations. The amount of phosphate adsorbed by the rock powder, $\Delta P$ ($\mu mol\ g^{-1}$), is

calculated by comparing the initial (dosed) and final (equilibrium) soluble reactive phosphate concentrations in the solution in each test tube:

$$\Delta P = ([SRP]_i - [SRP]_f) \times \frac{0.03 \text{ L solution}}{0.1 \text{ g rock powder}} \quad (1)$$

Here $[SRP]_i$ and $[SRP]_f$ are the soluble reactive phosphate concentrations for the initial and final solutions, respectively. Any "missing" phosphate is assumed to have adsorbed to the rock powder. For a given rock sample and water type, $\Delta P$ is plotted against $[SRP]_f$ to form its sorption isotherm curve. Various empirical and theoretical models are used to explain phosphate sorption behavior, and their defining equations reveal different aspects of the sorption behavior of the system when experimental data is fit to their parameters. The modified Freundlich isotherm equation is:

$$\Delta P + NAP = K_f [SRP]_f^n \quad (2)$$

where NAP (μmol $g^{-1}$) is the native adsorbed inorganic phosphate; the strength of the bond between phosphate and the mineral surface is inversely proportional to the Freundlich exponent in (Yakubu et al. 2008); and the Freundlich coefficient, $K_f$, indicates the relative adsorption capacity of the mineral surface. A high $K_f$ indicates a high rate of phosphate removal from solution (Yakubu et al. 2008).

The distribution coefficient, $K_d$ (L $g^{-1}$), is a measure of the buffer intensity and it can be calculated as:

$$K_d = n K_f [EPC_o]^{n-1} \quad (3)$$

where $EPC_o$ is equilibrium zero concentration, the phosphate concentration at which no net adsorption or desorption occurs (Zhang and Huang 2011). The $EPC_o$ is the value of $[SRP]_f$ at $\Delta P = 0$. The Langmuir sorption model assumes that there are a finite number of monolayer sorption sites on the mineral surface. The isotherm curve begins to flatten when adsorption sites become saturated; in other words, the mineral surfaces adsorb a smaller proportion of higher phosphate doses. The maximum monolayer sorption capacity, $P_{max}$, can be modeled as:

$$\Delta P = \frac{K_{eq}\, P_{max}\, [SRP]_f}{1 + K_{eq}\, [SRP]_f} \quad (4)$$

where the Langmuir constant $K_{eq}$ ($\mu M^{-1}$) indicates the affinity of phosphate for the adsorption sites. We fit these curves to data from our sorption isotherm experiments and estimated parameters values so as to evaluate a broad variety of sorption characteristics for a given aquifer solid when immersed in freshwater versus saltwater.

## Results

**Rock composition.** Composition results for the twelve samples from different elevations delineate distinct compositional patterns for the three geologic formations (Figure 3). All samples were low in phosphorus content, and all but two samples were low in iron. The Miami Limestone was particularly low in loosely adsorbed inorganic phosphate (mean value of $0.018 \pm 0.0009$ μmol $g^{-1}$), and was the only formation in which organic exceeded inorganic in terms of loosely adsorbed phosphate. The Fort Thompson Formation exhibited the greatest contrast between organic and inorganic loosely adsorbed phosphate. In the Fort Thompson Formation loosely adsorbed inorganic phosphate and total sedimentary phosphorus both increased with depth. The Tamiami Formation exhibited approximately three times the total

sedimentary phosphorus (mean value of 7.7 ± 1.02 μmol $g^{-1}$) as the other two formations (mean values were 1.44 ± 0.08 and 2.68 ± 1.8 μmol $g^{-1}$for Miami Limestone and Fort Thompson Formation, respectively). Based on the pattern of composition among the three geologic formations, the rock sample at the base of the Fort Thompson (sample 9) appears to have some commonality with the underlying Tamiami Formation in terms of its relatively high values of both loosely adsorbed organic phosphate and total sedimentary phosphate.

The samples with highest loosely adsorbed inorganic phosphate were samples 8 and 12 (0.105 ± 0.001 μmol $g^{-1}$and 0.096 ± 0.001 μmol $g^{-1}$, respectively), despite the fact that the sample from 8 had much lower total sedimentary phosphate than sample 12 (2.8 vs. 8.2 μmol $g^{-1}$ for samples 8 and 12, respectively). Sample 8 also had less carbonate-bound iron than sample 12 (14.4 vs. 26.5 μmol $g^{-1}$ for samples 8 and 12, respectively). The carbonate-bound iron was moderately high in sample 3 (40 μmol $g^{-1}$) and very high in sample 11 (118 μmol $g^{-1}$); all other samples exhibited less than 27 μmol $g^{-1}$, with the lowest being in the Miami Limestone samples (5 μmol $g^{-1}$).

**Sorption isotherm analysis.** Sorption behavior correlated more strongly with water type than composition for the seven rock samples for which equilibrium batch experiments were conducted (Figure 4). All rock layers exhibited a high contrast between the two water types in affinity of phosphate for adsorption sites ($K_{eq}$). Two samples exhibited particularly high contrast between the water types, in freshwater samples 2 and 8 exhibited especially high adsorption capacity and native adsorbed phosphate ($K_f$ and NAP), and sample 1 exhibited particularly high freshwater bond strength ($n^{-1}$), and sample 8 had particularly high buffer intensity ($K_d$). The two Tamiami Formation samples included in the sorption isotherm experiments (samples 11 and 12) exhibited

the least contrast in sorption behavior by water type, particularly with respect to $K_f$, $n^{-1}$, NAP, and $K_d$. In most samples, native adsorbed inorganic phosphorus (NAP) was high in freshwater, and was zero or near zero in saltwater, which is consistent with other work on bedrock and carbonate sediment that compared freshwater and saltwater sorption behavior (Flower et al. 2016; Flower 2016). The inverse of the Freundlich exponent n is an indication of the surface bond strength; it was much higher in freshwater compared to saltwater for all samples (1.4 to 21 times higher). Only the maximum monolayer sorption capacity, $P_{max}$, varied more by rock than water type (Table 3).

**Column experiments.** The first three column experiments were conducted with sample 12 from the Tamiami Formation (Figure 5). Freshwater leachate phosphate concentration was low (0.22 ± 0.08 µM phosphate for the three experiments combined), but still higher than the influent freshwater (0.050 µM phosphate). In the first leachate sample for which saltwater could be detected (using conductivity as tracer), phosphate concentration increased by 250%, 400%, and 280% for column experiments one, two, and three, respectively. Leachate phosphate concentration then rapidly increased in proportion to conductivity, peaking at 0.87, 1.67, and 0.98 µM for column experiments one, two, and three, respectively (Figure 5 omits the two data points that exceeded 1 µM, both of which were for column experiment 2). After the first pore volume of saltwater passed through the column, leachate phosphate concentration began to decline relatively steeply. The passage of an additional 4.4 pore volumes (44 mL) of saltwater through the columns caused phosphate concentration to decreases by 26%, 35%, and 25% for column experiments one, two, and three, respectively. Because the inflow water was changed to freshwater at that point, it is not known how phosphate concentration would have changed with continued saltwater flow. The phosphate concentration exhibited a slope of -0.0037 within

continued saltwater flow, and steepened slightly to -0.0048 when conductivity began to decline with the return of freshwater. When leachate was again pure freshwater, phosphate concentration returned to its former freshwater baseline (0.23 ± 0.07 µM).

The aquifer solids underwent a second influx of saltwater in the first two column experiments; again phosphate desorbed from the aquifer solids, but at a slower rate and with a dampened peak (27% and 16% less than the first peak, for experiments 1 and 2 respectively) (see Figure 5). Column experiments 4 and 5 were conducted with a second set of aquifer solids, sample 8 from the Fort Thompson Formation (Figures 6 and 7). In these experiments there was only one change to saltwater (Table 2). Compared to sample 12, freshwater leachate phosphate concentration was lower for sample 8 (0.16 ± 0.10 µM for the two column experiments combined). With the change of inflow from freshwater to saltwater, leachate phosphate concentration rose rapidly in proportion to conductivity, peaking at 0.93 ± 0.002 µM and 0.77 ± 0.002 µM (for column experiments 4 and 5 respectively). The main difference in column experiment 4 from the previous column experiments was that full strength saltwater leachate did not exhibit an overall decline in phosphate concentration. Instead, leachate phosphate concentration averaged 0.69 ± 0.05 µM until the return of freshwater (Figure 6).

Column experiment 5 was designed to examine desorption behavior with sustained flow of saltwater; 60 mL of freshwater was followed by 200 mL of saltwater (Table 2). The resulting desorption curve (Figure 7) can be broken into three main sections demarcating changes in slope: (1) rapid increase in phosphate concentration starting with the first detection of saltwater and continuing to full strength saltwater, for a total of 2.4 pore volumes (linear regression $R^2 = 0.8547$, $p < 0.00001$); (2) a relatively steep initial decline in phosphate concentration as saltwater flow continued for 5.2 pore volumes (linear regression $R^2 = 0.80$, $p < 0.00001$); and

(3) the remaining 14 pore volumes of saltwater flow, for which phosphate concentration was relatively stable at 0.51 ± 0.06 µM. A linear regression analysis of the third section reveals a weak negative trend (Pearson r = -0.39) that is significant at $p$ <0.02 and but has a high degree of variability ($R^2$ = 0.15).

For column experiment 5 we calculated a total mass balance of 0.115 ± 0.0002 µmoles phosphate desorbed, or 0.003 µmol phosphate per gram of aquifer solids, by taking the area under the curve using four methods (rectangular; trapezoidal; Simpson's rule; and the sum of the definite integral of each of the three linear regression equations). We made a calculation for the additional moles that would desorb if the trend continued, by projecting the third linear regression equation forward to the point where phosphate concentration goes to zero. This calculation projected an additional 0.199 µmol phosphate of expected desorption, which would take an additional 18 hours. The cumulative total of observed and projected phosphate desorption is 0.007 µmol phosphate per gram aquifer solids. This is approximately 7% of the measured loosely adsorbed inorganic phosphate of sample 3 (0.096 ± 0.002 µmol $g^{-1}$). (A caveat is that our loosely adsorbed inorganic phosphate measurements were conducted on a smaller grain size of the same rock, and the subsequent increase in surface area is likely to have resulted in higher measurement of loosely adsorbed inorganic phosphate.)

Although the samples chosen for the column experiments had similar measurements of loosely adsorbed inorganic phosphate (approximately 0.1 µmol $g^{-1}$), sample 12 from the Tamiami Formation had 7.5 times the loosely adsorbed organic phosphate, three times the total sedimentary phosphorus, and double the carbonate-bound iron, compared to sample 8 from the Fort Thompson Formation. In equilibrium batch experiments sample 12 exhibited a muted

contrast between freshwater and saltwater sorption behavior: to 85% lower adsorption capacity ($K_f$), 86% lower buffer intensity ($K_d$), 25% lower adsorption site affinity ($K_{eq}$), 80% lower bond strength ($n^{-1}$), and much lower native adsorbed phosphate (0 vs. 9.5 μmol $g^{-1}$ NAP), compared to sample 8. In terms of sorption isotherm parameters, sample 12 only exceeded sample 8 in terms of maximum monolayer sorption capacity ($P_{max}$ 13% higher).

**Discussion**

This study was designed to investigate for the first time the phosphate desorption kinetics of carbonate aquifer solids with low and moderate/high phosphorus content in response to salinization and freshening. Although our rock samples did not offer us the opportunity to investigate desorption behavior with moderate/high phosphorus content in this study, we were surprised to find that even rocks with very low amounts of loosely adsorbed inorganic phosphate and total sedimentary phosphorus exhibited rapid and intense phosphate desorption in response to an influx of saltwater.

Phosphate desorption is considered to be relatively rapid, e.g., 20-30 minutes for phosphate-loaded calcite and aragonite (Millero et al. 2001), but the rate of initiation has been unknown. By taking samples at 1-2 minute (mL) intervals as the inflow water turned from fresh to salty we were able to examine the initiation of desorption in high temporal resolution. In all of our column experiments phosphate desorption occurred with the first exposure to saltwater, even when leachate was sampled at 1 mL resolution (1 mL $min^{-1}$ flow rate).

Our conceptual model was that a single aquifer would be likely to exhibit a range intensity of saltwater-induced phosphate desorption depending on stratigraphic layer, due to influences on sorption behavior such as contrasting chemical composition among rock layers.

Based on experiments involving rocks pre-loaded with phosphorus (Corbett et al. 2000; Millero et al. 2001; Price et al. 2010), we consider it likely that rocks with greater amounts of loosely adsorbed inorganic phosphate would undergo more intense saltwater-induced phosphate desorption. Conversely, phosphate desorption may be minimal in rocks with significantly less loosely adsorbed inorganic phosphate than the two we tested.

Although our 12 samples provided a snapshot of compositional variability in the Biscayne aquifer at the G-3784 test corehole, all were low in phosphorus. The exceptionally low Miami Limestone phosphorus content was consistent with measurements of two limestones from the tops of two well cores in a different part of the Biscayne aquifer (a loosely adsorbed inorganic phosphate of 0.01-0.02 μmol $g^{-1}$ and total sedimentary phosphorus of 1.2-1.7 μmol $g^{-1}$) (Flower 2016). The total sedimentary phosphorus content of our samples from the Tamiami Formation (7.7 μmol $g^{-1}$) was three times that of the other units, but was lower than expected since parts of the Tamiami Formation have been found to have up to 3% phosphate grains (Cunningham et al. 2001). The average phosphorus content of continental rock has been given as 21 μmol $g^{-1}$ by Rudnick and Gao (2003). In addition, our Tamiami Formation samples exhibited a low loosely adsorbed inorganic phosphate value (0.072 ± 0.017 μmol $g^{-1}$), only slightly higher than the Ft Thompson samples (0.068 ± 0.019 μmol $g^{-1}$). For comparison, such values fall within the low end of loosely adsorbed inorganic phosphate measured in 40 samples of Florida Bay sediment (0.02 – 0.60 μmol $g^{-1}$), and below the range measured in 17 samples of Everglades soils (0.68 – 3.04 μmol $g^{-1}$) (Chambers and Pederson 2006; Zhang and Huang 2007).

The similarly rapid and intense desorption observed for samples 8 and 12 is striking given the differences between the two. In our equilibrium batch experiments all seven of the rock samples we tested responded to saltwater immersion with drastically reduced sorption isotherm

parameters compared to freshwater (Figure 4). Putting the equilibrium and kinetic results together, it appears that low saltwater sorption isotherm parameters predict rapid and intense desorption in response to an influx of saltwater. Freshwater sorption parameters may provide an indication as to persistence of desorption. Sample 12 exhibited sorption parameters in freshwater that were not much higher than in saltwater, and desorption declined substantially even as saltwater flowed. The persistent saltwater-induced desorption observed for sample 8 may be associated with its greater loosely adsorbed inorganic phosphate (Figure 3), and its higher freshwater adsorption capacity, native adsorbed phosphate, and buffer intensity (Figure 4).

Iron content was not associated with greater affinity for adsorbing phosphate as we had expected; the three samples highest in iron (3, 11, and 12) were among the samples with the least difference between freshwater and saltwater isotherm parameters. Iron content was found to be an important driver of sorption behavior in samples with low phosphorus content in a study of calcareous sediments from Florida Bay (Flower 2016; Zhang and Huang 2007). Further work is needed to better understand what factors affect the duration of seawater-induced desorption.

The narrowness of the first extreme phosphate release with saltwater influx in our experiments is consistent with phosphate being predominantly active at the ion exchange front of saltwater intrusion, which is also where sodium and calcium ions undergo cation exchange. The results in this study add a kinetic dimension to our previous study of carbonate rock from a different part of the Biscayne aquifer, wherein the sorption efficiency of the bedrock decreased logarithmically beginning with mixtures containing $\leq$ 0.5% saltwater, a part of the mixing continuum which would still be classified as fresh water (Flower 2016). A sharp peak of phosphate desorption confined to the first pore volume has been observed in cation exchange studies, where it has been described as “the snowplow effect” (Starr and Parlange 1979). This

effect is thought to occur because the ratio of ions in the influent saltwater greatly exceeds the available exchange sites on the solid surfaces, causing most exchange sites to be filled rapidly when first exposed to saltwater. Although we did see a relatively narrow initial peak in most of our column experiments the decline in phosphate desorption was more gently sloping than the decline in conductivity, spanning many pore volumes.

However, the mechanism driving seawater-induced phosphate desorption is as yet uncertain. There is general consensus that phosphate adsorption on oxide and clay minerals involves ligand exchange between phosphate anions and a reactive surface hydroxyl on positively charged exchange sites (Goldberg and Sposito 1985). Seawater-induced phosphate desorption may involve negatively charged exchange sites. Phosphate adsorption on pure phase calcium carbonates (calcite and aragonite) may increase in the presence of magnesium and calcium ions due to bridged complexes such as $>CO_3$—Mg— $PO_4$ and $>CO_3$—Ca—$PO_4$ bonds (Millero et al. 2001). An analogous set of bridged reactions is thought to occur on iron oxide compounds such as goethite (Gao and Mucci 2003). The sulfate in seawater may result in sulfate ion pairs ($MgSO_4$ and $CaSO_4$), decreasing the activity of magnesium and calcium, and thereby reducing phosphate adsorption (Millero et al. 2001). It has also been suggested that sulfate ions compete directly with phosphate for positive (calcium) sorption sites on calcium carbonate, further weakening phosphate adsorption in saltwater (Millero et al. 2001). Further work is required to better understand the precise mechanism driving seawater-induced phosphate desorption; data from this study will be used as input into a geochemical model for this purpose.

In the column experiments with sample 8 (column experiments 4 and 5) a third phase of phosphate desorption was evident, in which phosphate concentration in leachate appeared to stabilize or decline extremely gradually. Full strength saltwater leachate exhibited plateau of

phosphate concentration of 0.69 ± 0.05 µM and 0.51 ± 0.06 µM for column experiments 4 and 5, respectively. The transition to a quasi-stable phosphate desorption phase sample 8 could indicate a transition from low to high binding energy exchange sites. It is generally believed that some types of reactive sites on the solid surface, such as amorphous iron oxides on carbonate sediments, have stronger affinity for phosphate (Zhang and Huang 2007). As phosphate from the ambient water progressively adsorbs to the surface, phosphate binds to the strongest affinity sites available; conversely it is plausible that as desorption proceeds, phosphate vacates the lowest affinity sites first. Our sorption isotherm experiments support the possibility that sample 8 had this interpretation and add detail. Phosphate affinity for adsorption sites ($K_{eq}$) and phosphate-mineral surface bond strength (the inverse of Freundlich exponent n) were both much greater in sample 8 compared to sample 12.

Our isotherm parameters are similar to those found for two samples of bedrock from a southwestern part of the Biscayne aquifer, with the exception that the maximum monolayer sorption capacity values ($P_{max}$) in the present study are higher (Flower 2016). Our freshwater Freundlich coefficients ($K_f$), which indicate the relative rate of phosphate removal from solution, are similar to those determined for sediments from the freshwater wetland and pinelands in the Everglades (Zhou and Li 2001), and our saltwater Freundlich coefficients are within the range of values estimated for Florida Bay sediments (Zhang and Huang 2007).

Without further experimentation with flow rate, it is impossible to know if our aquifer solids could have raised the leachate phosphate concentration to higher concentrations than we observed. If the advective removal rate of desorbed phosphate is much faster than the phosphate desorption rate, phosphate concentration in the leachate will be much less than the equilibrium zero concentration ($EPC_o$). In other words, slower flow may raise the leachate phosphate

concentration (up to the $EPC_o$) and faster flow rate may lower it. Alternatively, it may be that the kinetics of phosphate desorption within our columns was very rapid compared to the advective phosphate removal rate. If this is the case, slowing the flow rate would not change the leachate phosphate concentration; raising the flow rate would be expected to lower the leachate phosphate concentration when the threshold is reached at which the advective phosphate removal exceeds seawater-induced phosphate desorption. Further column studies with varying flow rate would be necessary to determine if the stable leachate phosphate concentration we measured reflected a dynamic equilibrium phosphate concentration.

Given that we observed saltwater leachate phosphate concentrations of 0.5 µM and higher, we infer that seawater-induced phosphate desorption can be an important contributor to the phosphorus budget for the overlying ecosystem that subsequently receives the brackish groundwater as discharge. In phosphorus limited ecosystems all sources of phosphorus are important. Field experiments in the Everglades have found that a sustained rise of as little as 0.16 µM (5 ppb) in ambient surface water phosphate concentration doubled primary productivity and changed the vegetation composition (Gaiser et al. 2005; Noe et al. 2001). The total phosphorus criterion for surface water in the Everglades Protection Area is a long-term average of 0.3 µM (10 ppb) (NRC 2010). It would typically take considerably less phosphate to exceed this regulatory total phosphorus limit because dissolved organic phosphate and particulate phosphorus (both organic and inorganic) are also included in measurements of total phosphorus. Although vertical flow is impeded by semi-permeable layers in parts of the Biscayne aquifer, including at the G-3784 test corehole (Cunningham et al. 2006; Cunningham et al. 2004), in other parts of the same aquifer brackish groundwater is known to discharge to the overlying mangrove estuary (Price et al. 2006; Spence 2011; Zapata-Rios and Price 2012).

The phosphate desorption events we observed were time-limited, i.e., they showed signs of waning phosphate desorption within the hours of study, but it is important to remember that the products of phosphate desorption were constantly exiting the system. In an aquifer undergoing incremental saltwater intrusion, a given parcel of intruding saltwater may take much longer to be removed by advection or another process. Here our equilibrium isotherm experiments on samples from seven of the rock samples add valuable information (Figure 3). In saltwater all rocks had (in comparison to their values in freshwater) lower native adsorbed phosphorus (NAP), lower adsorption capacity ($K_f$), lower buffer intensity ($K_d$), a weaker bond between phosphate ions and the mineral surface (high Freundlich exponent n), and a lower affinity of phosphate for the adsorption sites ($K_{eq}$) (Table 3). Thus, although saltwater-induced phosphate desorption would be an event of limited duration, the consequences to groundwater phosphate concentration would likely endure, in turn affecting overlying ecosystems when the brackish water ultimately discharges to the surface.

Our column experiments suggest that sorption dynamics within a carbonate aquifer may also shift rapidly in response to freshening, and our sorption isotherm experiments indicate that adsorption of excess phosphate to mineral surfaces would likely result. Oscillations of salinization and freshening have been observed in Biscayne aquifer wells (Prinos et al. 2014), even on short timescales (Kohout and Klein 1967). Such oscillations may cause alternating phosphate adsorption/desorption cycles unless removed from the system, e.g. by advection or microbial activity). We estimated that a given event of saltwater-induced phosphate desorption would run its course well short of exhausting the reserve of loosely adsorbed inorganic phosphate, leaving 93% on the mineral surfaces, based on our mass balance calculations. However, successive episodes of phosphate desorption may be less effective at desorbing

phosphate, as we showed in column experiments 1 and 2, in which freshening was followed by a second influx of saltwater (Figure 5).

## Conclusions

Our results support the hypothesis that saltwater-induced phosphate desorption occurs within carbonate coastal aquifers even in rocks with low phosphorus content. We found that the duration of saltwater-induced phosphate desorption varied between rocks; intensity waned within minutes in one case and remained elevated for hours in another. Once desorbed, phosphate ions can remain at an elevated concentration in saltwater due to the low buffering capacity of measured for all of our rock samples when immersed in saltwater. An incursion of saltwater into limestone in a coastal aquifer that had been immersed in fresh groundwater appears likely to raise ambient groundwater phosphate concentrations to a level high enough to affect the overlying estuary receiving brackish groundwater discharge.

**Acknowledgments.** Thanks to Kevin Cunningham of United States Geological Survey for assisting in the laboratory with lithologic descriptions, selection of intact Tamiami Formation specimens, and for providing access to G-3784 test corehole. Dr. René Price, Rafael Travieso and Edward Linden of Florida International University provided for field and laboratory support; and Charles Fischer of National Oceanic and Atmospheric Administration/Atlantic Oceanographic and Meteorological Laboratory assisted in sample analysis. We also wish to thank the associate editor and anonymous reviewer who provided detailed feedback, vastly improving the manuscript, particularly with regard to stratigraphy. This material is based upon work supported by the National Science Foundation through the Florida Coastal Everglades Long-Term Ecological Research program under Cooperative Agreements #DEB-1237517, #DBI-0620409, and #DEB-9910514. This is contribution number 823 from the Southeast Environmental Research Center at Florida International University.

## References


Barlow, P.M., and E.G. Reichard. 2010. Saltwater intrusion in coastal regions of North America. *Hydrogeology Journal* 18: 247-260.

Chambers, R.M., and K.A. Pederson. 2006. Variation in soil phosphorus, sulfur, and iron pools among south Florida wetlands. *Hydrobiologia* 569: 63-70.

Corbett, D.R., L. Kump, K. Dillon, W. Burnett, and J. Chanton. 2000. Fate of wastewater-borne nutrients under low discharge conditions in the subsurface of the Florida Keys, USA. *Marine Chemistry* 69: 99-115.

Cotecchia, V., G. Tazioli, and G. Magri. 1974. Isotopic measurements in research on seawater ingression in the carbonate aquifer of the Salentine Peninsula, southern Italy. In Isotope techniques in groundwater hydrology 1974, Vol. I. Proceedings of a symposium.

Cunningham, K.J., D. Bukry, T. Sato, J.A. Barron, L.A. Guertin, and R.S. Reese. 2001. Sequence stratigraphy of a south Florida carbonate ramp and bounding siliciclastics (late Miocene–Pliocene). *Geology and hydrology of Lee County, Florida: Florida Geological Survey Special Publication* 49: 35-66.

Cunningham, K.J., M.A. Wacker, E. Robinson, J.F. Dixon, and G.L. Wingard. 2006. A cyclostratigraphic and borehole-geophysical approach to development of a three-dimensional conceptual hydrogeologic model of the karstic Biscayne aqui fer, southeastern Florida. In U.S. Geological Survey Scientific Investigations Report 2005-5235, 69 p., plus CD.

Cunningham, K.J., M.A. Wacker, E. Robinson, C.J. Gefvert, and S.L. Krupa. 2004. Hydrogeology and ground-water flow at Levee 31°N, Miami-Dade County, Florida, July 2003 to May 2004. In U.S. Geological Survey Scientific Investigations Map I-2846, 1 sheet.

D'Angelo, E., J. Crutchfield, and M. Vandiviere. 2001. Rapid, sensitive, microscale determination of phosphate in water and soil. *Journal of Environmental Quality* 30: 2206-2209.

Fitterman, D.V. 2014. Mapping saltwater intrusion in the Biscayne aquifer, Miami -Dade County, Florida using transient electromagnetic sounding. *Journal of Environmental and Engineering Geophysics* 19: 33-43.

Flower, H., M. Rains, D. Lewis, J.-Z. Zhang, and R. Price. 2016. Control of phosphorus concentration through adsorption and desorption in shallowgroundwater of subtropical carbonate estuary. *Estuarine, Coastal and Shelf Science* 169: 238-247.

Flower, H.R., Mark; Zhang, Jia-Zhong; Lewis, David; Price, René. 2017. Saltwater intrusion as potential driver of phosphorus release from limestone bedrock in a coastal aquifer. *Estuarine, Coastal and Shelf Science* 185: 166-176.

Froelich, P.N. 1988. Kinetic control of dissolved phosphate in natural rivers and estuaries: A primer on the phosphate buffer mechanism. *Limnology and oceanography* 33: 649-668.

Gaiser, E.E., J.C. Trexler, J.H. Richards, D.L. Childers, D. Lee, A.L. Edwards, L.J. Scinto, K. Jayachandran, G.B. Noe, and R.D. Jones. 2005. Cascading ecological effects of low-level phosphorus enrichment in the Florida Everglades. *Journal of Environmental Quality* 34: 717-723.

Gao, Y., and A. Mucci. 2003. Individual and competitive adsorption of phosphate and arsenate on goethite in artificial seawater. *Chemical geology* 199: 91-109.

Goldberg, S., and G. Sposito. 1985. On the mechanism of specific phosphate adsorption by hydroxylated mineral surfaces: A review. *Communications in Soil Science & Plant Analysis* 16: 801-821.

Huang, X.-L., and J.-Z. Zhang. 2009. Neutral persulfate digestion at sub-boiling temperature in an oven for total dissolved phosphorus determination in natural waters. *Talanta* 78: 1129-1135.

Kohout, F., and H. Klein. 1967. Effect of pulse recharge on the zone of diffusion in the Biscayne aquifer. In International Association of Scientific Hydrogeology Symposium, Haifa, Israel, pub, 252-270.

Millero, F., F. Huang, X. Zhu, X. Liu, and J.-Z. Zhang. 2001. Adsorption and desorption of phosphate on calcite and aragonite in seawater. *Aquatic Geochemistry* 7: 33-56.

Moore, W.S. 1999. The subterranean estuary: a reaction zone of ground water and sea water. *Marine Chemistry* 65: 111-125.

Noe, G.B., D.L. Childers, and R.D. Jones. 2001. Phosphorus biogeochemistry and the impact of phosphorus enrichment: why is the Everglades so unique? *Ecosystems* 4: 603-624.

NRC. 2010. *National Research Council: Progress Toward Restoring the Everglades: The Third Biennial Review*. Washington, DC: The National Academies Press, 326 p.

NRC. 2014. *National Research Council: Progress Toward Restoring the Everglades: The Fifth Biennial Review*. Washington, DC: The National Academies Press, 302 pp.

Price, R.M. 2001. Geochemical determinations of groundwater flow in Everglades National Park, Ph.D. Dissertation, University of Miami, 307 pp.

Price, R.M., and J.S. Herman. 1991. Geochemical investigation of salt-water intrusion into a coastal carbonate aquifer: Mallorca, Spain. *Geological Society of America Bulletin* 103: 1270-1279.

Price, R.M., M.R. Savabi, J.L. Jolicoeur, and S. Roy. 2010. Adsorption and desorption of phosphate on limestone in experiments simulating seawater intrusion. *Applied Geochemistry* 25: 1085-1091.

Price, R.M., P.K. Swart, and J.W. Fourqurean. 2006. Coastal groundwater discharge–an additional source of phosphorus for the oligotrophic wetlands of the Everglades. *Hydrobiologia* 569: 23-36.

Prinos, S.T., M.A. Wacker, K.J. Cunningham, and D.V. Fitterman. 2014. Origins and delineation of saltwater intrusion in the Biscayne aquifer and changes in the distribution of saltwater in Miami-Dade County, Florida. *U.S. Geological Survey Scientific Investigations Report 2014-5025, 101 p.* Rudnick, R., and S. Gao. 2003. 3.01 Composition of the continental crust. *Treatise on geochemistry* 3 The Crust: 1-64.

Ruttenberg, K.C. 1992. Development of a sequential extraction method for different forms of phosphorus in marine sediments. *Limnology and oceanography* 37: 1460-1482.

Slomp, C.P., and P. Van Cappellen. 2004. Nutrient inputs to the coastal ocean through submarine groundwater discharge: controls and potential impact. *Journal of Hydrology* 295: 64-86.

Spence, V. 2011. Estimating groundwater discharge in the oligohaline ecotone of the Everglades using temperature as a tracer and variable-density groundwater models, Masters Thesis, University of South Florida at Tampa, 36 pp.

Starr, J., and J.-Y. Parlange. 1979. Dispersion in soil columns: The snow plow effect. *Soil Science Society of America Journal* 43: 448-450.

Suzumura, M., S. Ueda, and E. Sumi. 2000. Control of phosphate concentration through adsorption and desorption processes in groundwater and seawater mixing at sandy beaches in Tokyo Bay, Japan. *Journal of oceanography* 56: 667-673.

USGS. 2003. Lithologic and Geophysical Log for G-3784. U. S. Geological Survey, Center for Water and Restoration Studies, Miami, Florida, 1 sheet.

Wang, Q., and Y. Li. 2010. Phosphorus adsorption and desorption behavior on sediments of di fferent origins. *Journal of Soils and Sediments* 10: 1159-1173.

Yakubu, M., M. Gumel, and A. Abdullahi. 2008. Use of activated carbon from date seeds to treat textile and tannery effluents. *African Journal of Science and Technology (AJST) Science and Engineering Series* 9: 39-49.

Zapata-Rios, X., and R.M. Price. 2012. Estimates of groundwater discharge to a coastal wetland using multiple techniques: Taylor Slough, Everglades National Park, USA. *Hydrogeology Journal* 20: 1651-1668.

Zhang, J.-Z., and X.-L. Huang. 2007. Relative importance of solid-phase phosphorus and iron on the sorption behavior of sediments. *Environmental Science and Technology* 41: 2789-2795.

Zhang, J.-Z., and X.-L. Huang. 2011. Effect of temperature and salinity on phosphate sorption on marine sediments. *Environmental Science and Technology* 45: 6831-6837.

Zhang, J.-Z., C. Kelble, and F.J. Millero. 2001. Gas-segmented continuous flow analysis of iron in water with a long liquid waveguide capillary flow cell. *Analytica Chimica Acta* 438: 49-57.

Zhang, J.Z., C.J. Fischer, and P.B. Ortner. 2004. Potential availability of sedimentary phosphorus to sediment resuspension in Florida Bay. *Global Biogeochemical Cycles* 18 (4) GB4008: 1-14.

Zhou, M., and Y. Li. 2001. Phosphorus-sorption characteristics of calcareous soils and limestone from the southern Everglades and adjacent farmlands. *Soil Science Society of America Journal* 65: 1404-1412.

**Table 1.** Lithologic descriptions of the rock samples used for this study, along with approximate elevations for the top, bottom, and midpoint for the interval from which each specimen was taken.

| Sample Number | Elevations in m NAVD88 | | | Lithologic Description (USGS 2003) | Geologic Formation |
|---|---|---|---|---|---|
| | Top | Bottom | Midpoint | | |
| 1 | 1.3 | -0.1 | 0.6 | Peloid grainstone/packstone | Miami Limestone |
| 2 | -1.0 | -1.2 | -1.1 | Peloid grainstone/packstone | |
| 3 | -1.9 | -2.4 | -2.1 | Mudstone/wackestone | Fort Thompson |
| 4 | -3.4 | -3.6 | -3.5 | Molluscan foraminiferal floatstone | Formation |
| 5 | -4.8 | -5.1 | -5.0 | Touching- vug pelecypod floatstone-mudstone with mollusks visible | |
| 6 | -6.3 | -6.6 | -6.5 | Skeletal wackestone-packstone | |
| 7 | -7.9 | -8.0 | -7.9 | Mudstone/wackestone | |
| 8 | -9.1 | -9.4 | -9.2 | Planorbella floatstone/rudstone | |
| 9 | -10.6 | -10.8 | -10.7 | Quartz-rich pelecypodal floatstone mudstone | |
| 10 | -12.4 | -13.3 | -12.9 | Peloidal grainstone-packstone | Tamiami |
| 11 | -17.6 | -18.1 | -17.8 | Shelley quartz sand with abundant mollusk shells (unconsolidated) | Formation |
| 12 | -24.9 | -25.2 | -25.1 | Shelley quartz sand with abundant mollusk shells (unconsolidated) | |

**Table 2.** Summary of column experiments.

| Sample | Geologic Formation | Column Experiment | Sieved Grain Size, mm | Sequence of Water inflow | Leachate Sample Size |
|---|---|---|---|---|---|
| 12 | Tamiami Formation | 1 | (not sieved) | Fresh (60 mL)<br>Salt (70 mL)<br>Fresh (70 mL)<br>Salt (70 mL)<br>Fresh (60 mL) | 2 mL |
| | | 2 | 1.0-1.4 | Fresh (60 mL)<br>Salt (70 mL)<br>Fresh (70 mL)<br>Salt (70 mL)<br>Fresh (60 mL) | 2 mL |
| | | 3 | 1.0-1.4 | Fresh (60 mL)<br>Salt (70 mL)<br>Fresh (60 mL) | 1 mL |
| 8 | Fort Thompson Formation | 4 | 1.0-1.4 | Fresh (60 mL)<br>Salt (70 mL)<br>Fresh (60 mL) | 2 mL |
| | | 5 | 1.0-1.4 | Fresh (60 mL)<br>Salt (200 mL) | 2 mL |

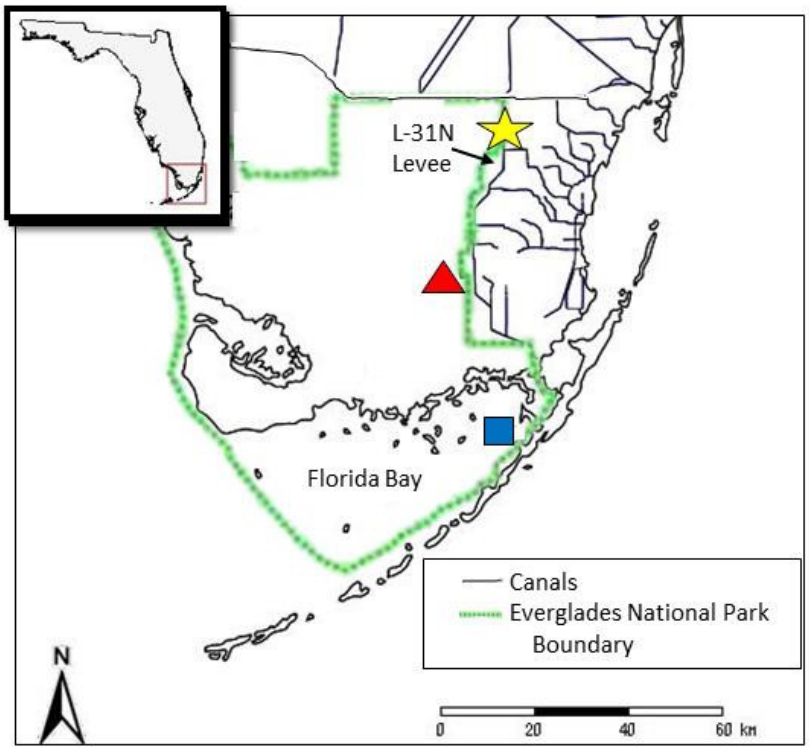


**Figure 1.** Location map showing the location of the G-3784 test corehole (yellow star), fresh groundwater well TSB15 (red triangle), and saltwater sampling site in Florida Bay (blue square).

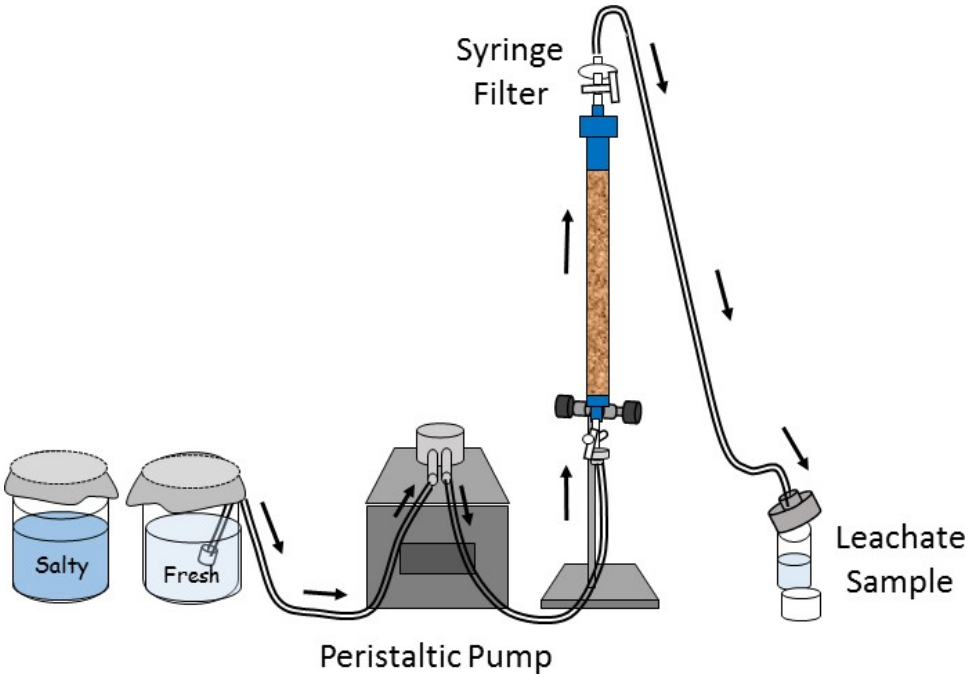


**Figure 2.** Schematic diagram of column apparatus.

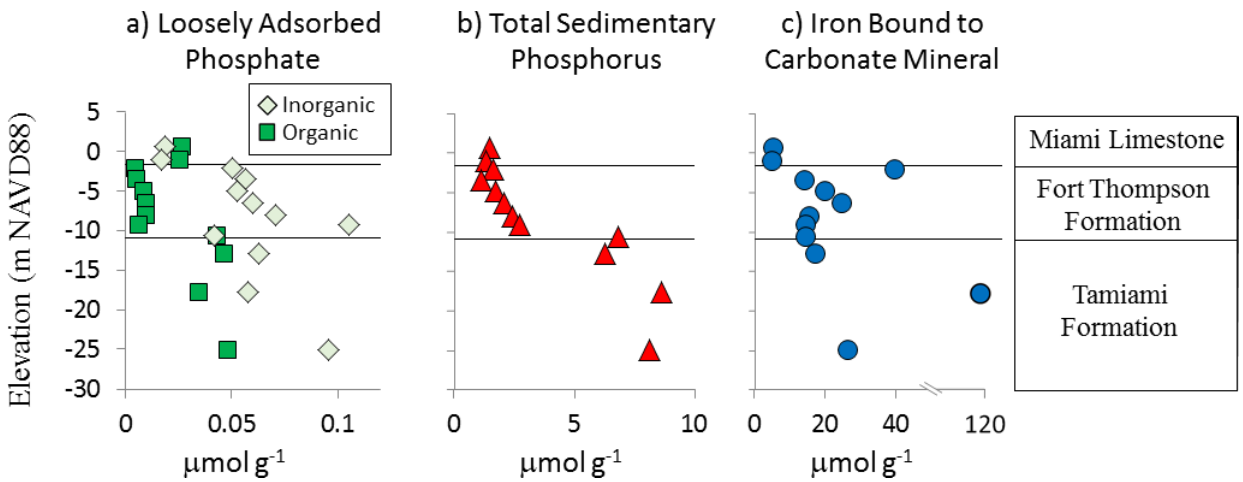


**Figure 3.** Rock composition: a) inorganic loosely adsorbed phosphate (pale green diamonds) and organic loosely adsorbed phosphate (dark green squares); b) total sedimentary phosphorus (red triangles); and c) iron bound to carbonate mineral (blue circles).

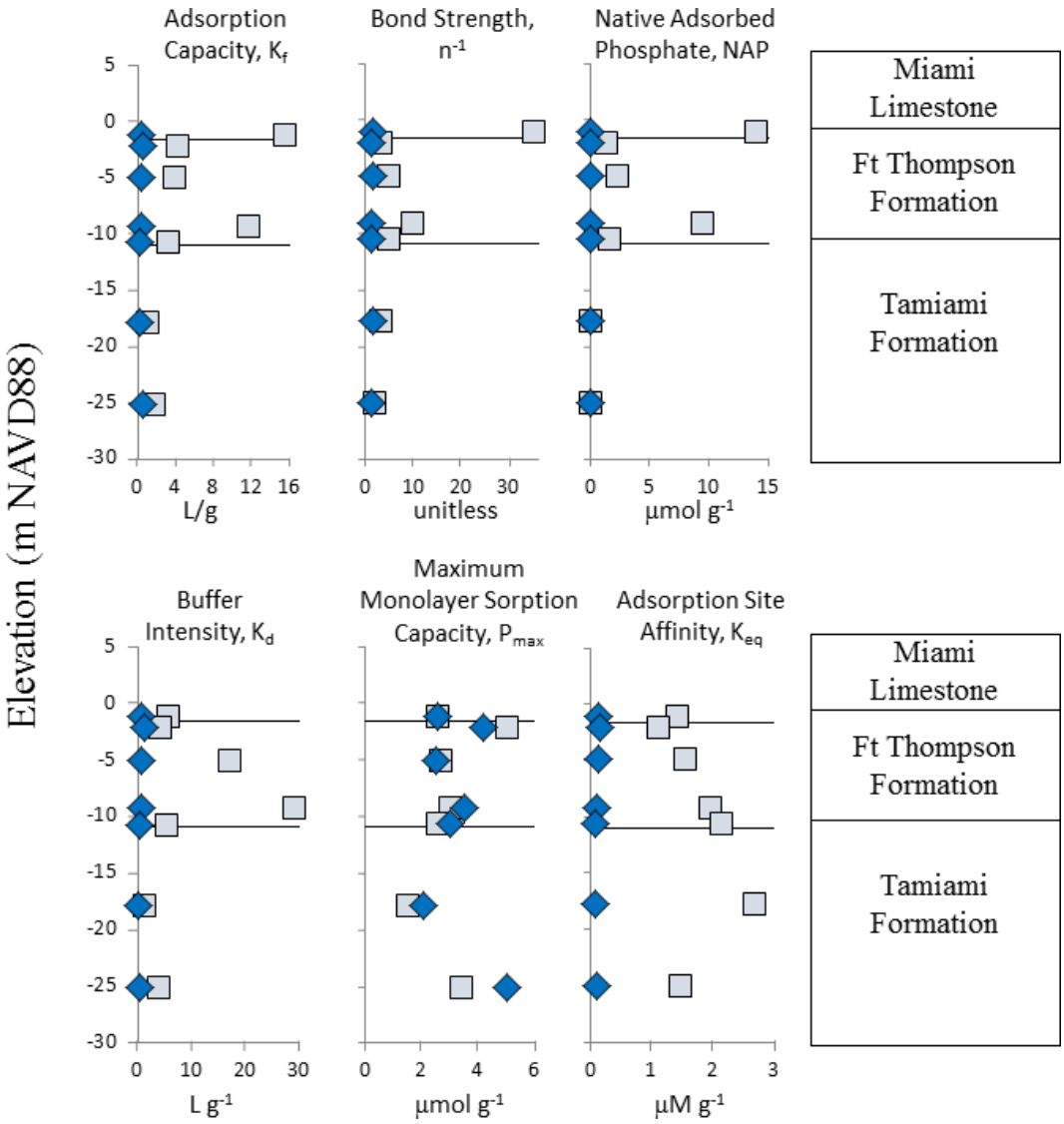


**Figure 4.** Isotherm sorption parameters as determined for seven aquifer samples in saltwater (dark blue diamonds) and in freshwater (pale blue squares).

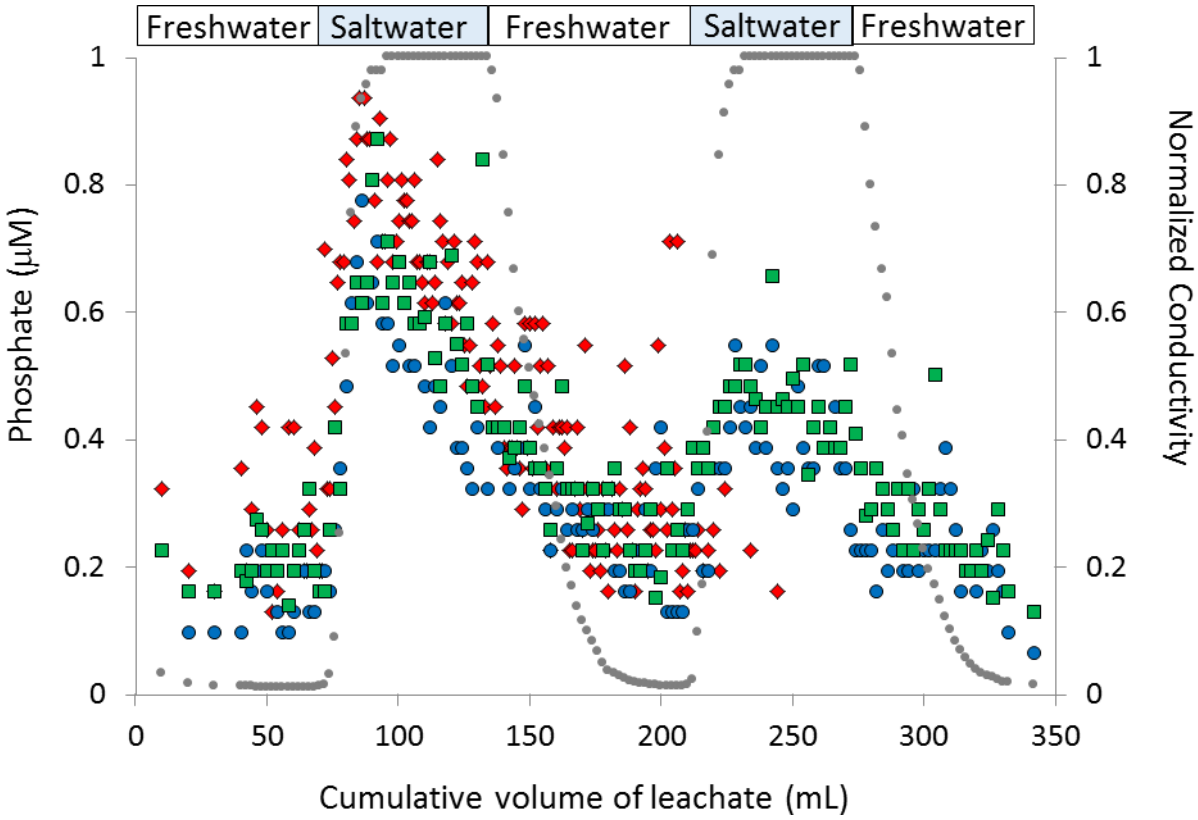


**Figure 5.** Column experiments involving sample 12: column experiment 1 (blue circles), 2 (green squares), and 3 (red diamonds); conductivity is shown as small gray circles.

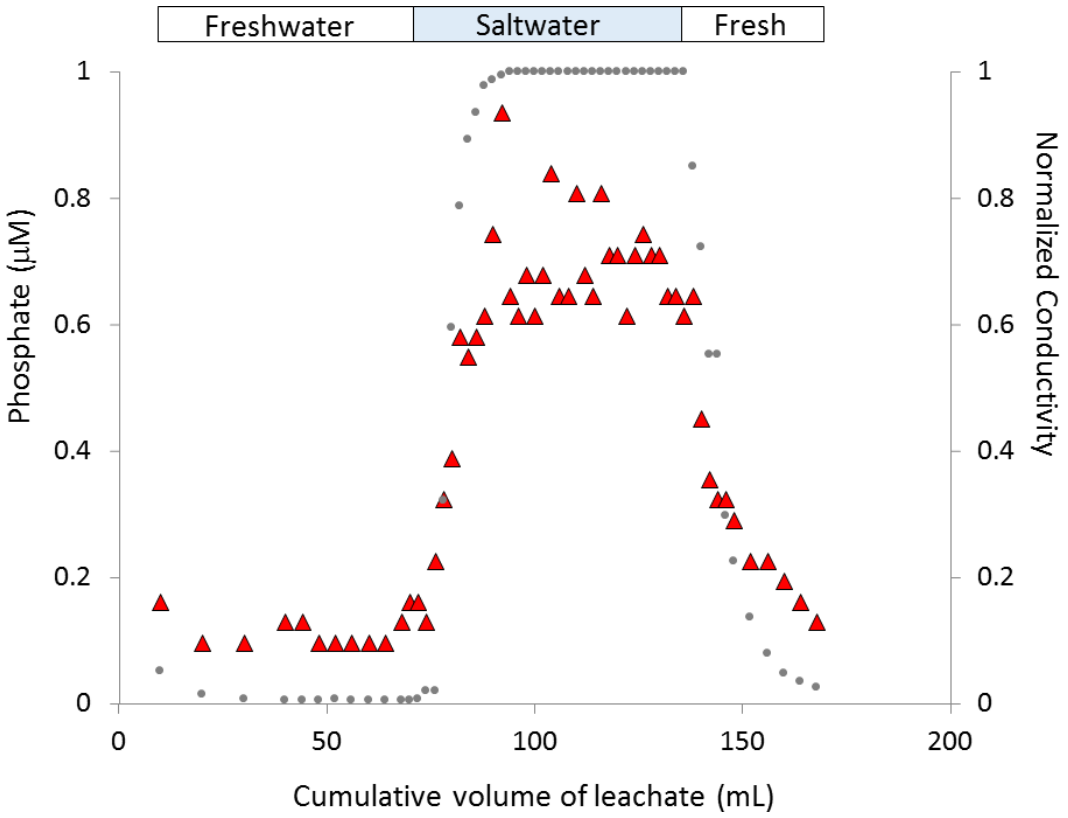


**Figure 6.** Column experiment 4 (sample 8).

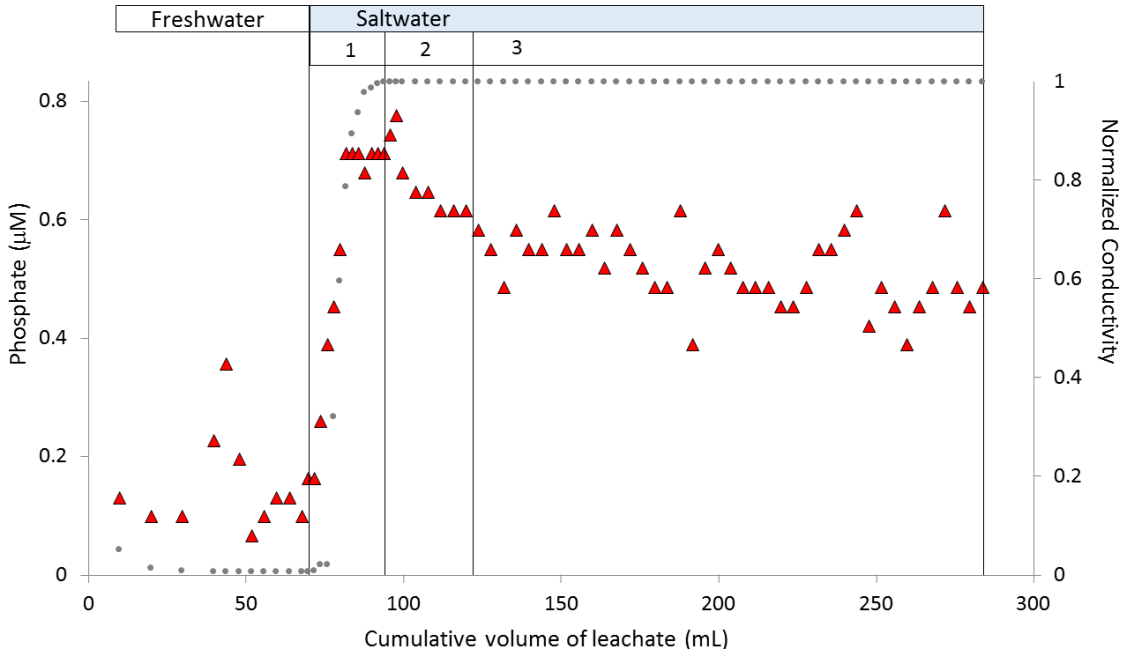


**Figure 7.** Column experiment 5 (sample 8) with sustained saltwater flow with the three phases of desorption indicated by the numbers.